Materials Science and Engineering A 527 (2010) 7689–7693

Contents lists available at ScienceDirect

Materials Science and Engineering A

journal homepage: www.elsevier.com/locate/msea

Fracture toughness of titanium foams for medical applications

Sadaf Kashef[a,*], Alireza Asgari[b], Timothy B. Hilditch[b], Wenyi Yan[c], Vijay K. Goel[d], Peter D. Hodgson[a]

[a] Institute for Technology Research and Innovation, Deakin University, Pigdons Road, Waurn Ponds, Victoria 3217, Australia
[b] School of Engineering, Deakin University, Waurn Ponds, Victoria 3217, Australia
[c] Department of Mechanical and Aerospace Engineering, Monash University, Clayton, Victoria 3800, Australia
[d] Engineering Center for Orthopedic Research Excellence, University of Toledo, Toledo, OH 43606, USA

ARTICLE INFO

Article history:
Received 11 June 2010
Received in revised form 10 August 2010
Accepted 16 August 2010

Keywords:
Titanium
Porosity
Open foam
Fracture toughness
Mechanical properties

ABSTRACT

The fracture behavior of titanium open foam is characterized and the R-curves of crack propagation from pre-cracks are measured. The crack growth has been optically observed, the measured initiation toughness, J_{IC}, has been analyzed and the effect of material morphology on the J_{IC} is discussed. The fracture toughness was found to be dependent on the expanding crack bridging zone at the back of the crack tip. The compact tension specimens also have some plastic collapse along the ligaments and it has shown that the titanium foam with a higher relative density is tougher. The non-uniform stressing within the plastic zone at the crack tip and the plastic collapse of cell topology behind the tip was found to be the primary cause of the R-curve behavior in low relative density titanium foams.

1. Introduction

Solid metal implants such as solid titanium with a porous coating have been used widely in the past to improve bone–implant interface. These porous coated implants with rough surfaces can prevent encapsulation and loosening of the implant and therefore promote long-term interface strength [1]. Solid titanium also has outstanding properties of high strength, low weight, and exceptional corrosion resistance and can be used for a diverse range of medical implants. The disadvantage of this material for implantation is its high stiffness compared to the bone. When an implant is much stiffer than the bone, the stress is removed from the bone and causes reduction in the bone mass and therefore resorption of bone. This phenomenon is known as stress shielding [2–4]. For load bearing applications, biomaterials need to have a close stiffness to the bone as well as high strength and toughness. The matched stiffness will help to avoid the stress shielding problems [5,6].

In a previous study we have shown that titanium foam with relative density of about 0.40 has a close stiffness to several important bone types within the skeletal system [7]. Other than the foam's stiffness and strength, the fracture toughness of biomaterials is an important material property that needs to be examined prior to clinical studies. Sufficient fracture toughness is necessary to prevent the prostheses from fracture inside the human body.

Fracture mechanics testing indicates the amount of stress needed to propagate a pre-existing flaw, which is especially important in a foam material as it already includes many flaws because of its porous structure. At present there is limited literature on the mechanical properties of biocompatible titanium foams. Imwinkelried [8] has studied mechanical properties via compression, tension, and classical fatigue testing using the S/N approach, on titanium foams. Teoh et al. have studied the effect of pore sizes on the fracture toughness of titanium foams with relative densities of 0.915 and 0.65 compacted at 0.17 and 0.62 GPa [9]. The fatigue behavior of titanium foams must be considered as they are very important in classifying the potential in orthopedic applications. However, to date, no advanced fracture mechanics study on low relative density titanium foams has been reported.

There are multiple processes that have emerged on titanium foam manufacturing, such as plasma-spray method with chemical and thermal treatments [10], hot isostatic pressed method backfilled with argon gas [11,12], Mg particles used as spacer [13], directional freeze-casting [14], and powder metallurgy method [15]. The latter method [15] using ammonium hydrogen bicarbonate particles as the spacer to fabricate porous metals as implant material has been applied here. This method has been used for our purpose as it is an appropriate technique for making foams from materials with high melting point such as titanium. Another advantage is that the pore distribution and pore parameters are also controllable with this simple method.

In this study the fracture toughness of titanium foams manufactured via the powder metallurgy process with variable high

* Corresponding author. Tel.: +61 3 5227 3359; fax: +61 3 5227 1103.
E-mail address: skas@deakin.edu.au (S. Kashef).

0921-5093/$ – see front matter © 2010 Elsevier B.V. All rights reserved.
doi:10.1016/j.msea.2010.08.044

Nomenclature

a_i	crack size at the end of an unloading/reloading sequence
b_i	uncracked ligament size at the end of an unloading/reloading sequence
A_{pl}	area of the plastic deformation in load–displacement diagram
Δa	crack extension
B	specimen thickness
E'	plane strain Young's modulus
EPFM	elastic–plastic fracture mechanics
J	J-integral (measurement of fracture toughness using EPFM)
J_{IC}	initiation fracture toughness
J_{pl}	J-integral of the plastic deformation
K	stress intensity factor
K_{IC}	plane strain fracture toughness
P	load
P_i	current load during the test
u	displacement
ν	Poisson's ratio
W	width of the specimen

porosities are discussed in terms of cellular structure and edge. The initiation toughness, J_{IC}, was measured and used to calculate the fracture toughness, K_{IC}, of the foams. The fractured compact tension titanium samples were analyzed by scanning electron microscopy (SEM). These values are compared against a range of skeletal components from literature.

2. Experimental procedures

2.1. Specimen materials and manufacturing

To produce open porous titanium material, the sintering of compacted mixtures of metal powder and space holder material, is one of the most promising methods, which can produce pore sizes from micrometres to millimetres [16]. The space holder method has been applied by Teoh et al. [9], Wen et al. [15], Imwinkelried [8], and Kashef et al. [7].

Commercially available titanium powder was used as metal powder. Titanium powder with the purity of 99.9%, average particle size of 45 μm, and irregular morphology was used. Ammonium bicarbonate, NH_4HCO_3 was used as space holder material for fabrication of metal foams. This powder is white with angular shape. The particles with purity of 99.0% were chosen with the size of 500–800 μm by sieving as this fraction of space holder generates suitable pores for bone ingrowth. The spacer material was chosen based on its chemical properties such that the spacer decomposes totally at a low temperature.

To get open pore with required properties, powder, green body, and sintering processes should be controlled. The production steps may be listed as [7]:

1. Mixing of the fine titanium powder with the space holder substance.
2. Pressing of a green body under 200 MPa pressure at room temperature.
3. Removal of the space holder by heat treatment at 100 °C for 10 h.
4. Sintering at high temperature of 1120 °C for 7 h by using vacuum furnace.

The relative density values were taken by weighing the samples. Titanium foams with relative densities of 0.30 (70% porosity) and 0.40 (60% porosity) were investigated here. The compact tension specimens measuring 16 mm × 15.36 mm × 6.4 mm (Fig. 1) were wire cut from 44 mm × 16 mm × 6.4 mm foam panels and then pre-cracked as explained in ASTM E1820-08, the standard test method for measurement of fracture toughness of metallic materials [17]. The advantages of wire cut are its small kerf to cut through softer materials, and its precise cut. The disadvantages of this method are that the cutting is done at slower speed and it is rather expensive; however, it is an appropriate cutting technique for porous materials.

2.2. Fracture toughness test

The fracture toughness testing was performed at room temperature using a MTS servo-hydraulic testing machine at a displacement rate of 0.01 mm/s. In accordance with the ASTM E1820-08, this test method is for the opening mode (mode I) of loading. In this test method, a fatigue pre-cracked specimen was loaded to induce crack extension while continuously measuring force versus displacement.

There are two different procedures for measuring the crack extensions: the basic procedure and the resistance curve procedure. For basic procedure multiple specimens are used to obtain a single point initiation toughness value. The resistance curve procedure determines multiple points from a single specimen and the data are used to develop an R-curve. The resistance curve procedure was used for our purpose.

2.3. Plane strain and initiation fracture toughness

The initiation fracture toughness J_{IC} and the plane strain fracture toughness K_{IC} were measured using three repetitions of the single specimen method described in ASTM E1820-08. A key advantage of this method is the ability to estimate both the J-integral and the K_{IC} for the same specimen. The specimens were unloaded and reloaded during the tests. From the load P versus load-line displacement u response of the specimen, the J-integral versus crack extension Δa response was calculated and plotted. In addition, digital images of crack tip growth were taken from both sides of the samples. The crack tip growth was measured with reference to unit length markers on each sample. The average of crack length at front and back of the sample was used as the average physical crack size from image processing technique.

J-integral represents a way to calculate the strain energy release rate per unit fracture surface area of the material [18]. The J-integral can be divided into J-integral of elastic and J-integral of plastic (Eq. (1)).

$$J_{total} = J_{elastic} + J_{plastic} = \frac{(K_i)^2(1-\nu^2)}{E} + \left[J_{pl(i-1)} + \left(\frac{2.0 + 0.522 b_{i-1}/W}{b_{i-1}}\right)\frac{A_{pl(i)} - A_{pl(i-1)}}{B}\right] \times \left[1 - (1.0 + 0.76 b_{i-1}/W)\left(\frac{a_i - a_{i-1}}{b_{i-1}}\right)\right] \quad (1)$$

The Poisson ratio ν is assumed to be 0.3 [19] and E, the Young's modulus was found from the elastic unloading compliance technique of the compact tension specimens. W is specimen width, B is the specimen thickness, a_i is current crack size, $b_i = W - a_i$ is the current uncracked ligament, and A_{pl} is the plastic deformation area in load–displacement graph. The highlighted region in Fig. 2 represents the plastic area increment $(A_{pl(i)} - A_{pl(i-1)})$ for resistance

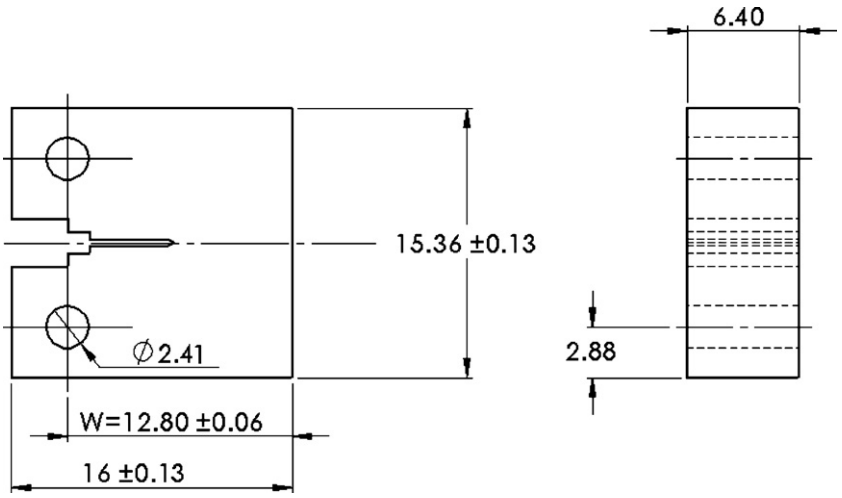

Fig. 1. Sketch and dimensions of compact tension titanium foam.

curve on a load–displacement diagram.

K_i is calculated from

$$K_i = \frac{P_i}{BW^{0.5}} f(a) \tag{2}$$

P_i is the maximum load, $a = a_i/W$, and

$$f(a) = \frac{(2+a)(0.886 + 4.64a - 13.32a^2 + 14.72a^3 - 5.6a^4)}{(1-a)^{3/2}} \tag{3}$$

The obtained J_{IC} was conventionally converted to K_{IC} by using Eqs. (4) and (5) [17].

$$K_{IC} = \sqrt{J_{IC} E'} \tag{4}$$

$$E' = \frac{E}{(1-\nu^2)} \tag{5}$$

E' is the plane strain Young's modulus.

At least eight samples were tested for each material. The crack extension measurement was carried out by image processing method and compliance technique according to section 8 of ASTM E1820-08. For both analysis techniques, each measurement was carried out at least three times for each sample within experimental error of less than 2%. The statistical analysis of the data has shown the degree of error below the 5% confidence level. Therefore, the data are statistically significant.

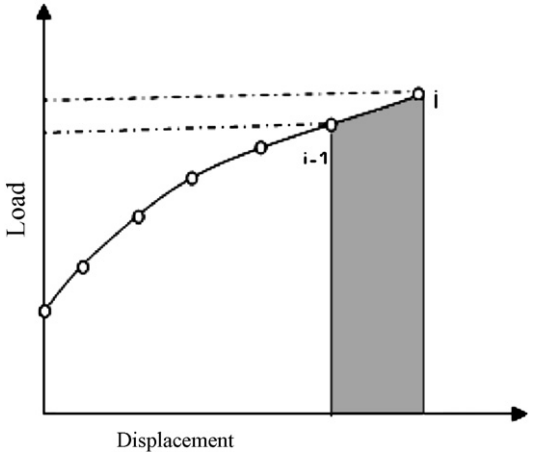

Fig. 2. Load–displacement graph for resistance curve J calculation.

3. Results

3.1. Analysis of mechanical behavior of foams

There are two parameters that affect the mechanical behavior of metallic foams. One is the properties of the solid material, and the other one is the architecture of cells such as density, size and their open or closed structure. The yield strength σ_{ys} was measured by tension testing to be 61.1 and 56.4 MPa for relative densities of 0.40 and 0.30, respectively. The density and elastic modulus of the cell walls chosen to be those of solid titanium, which are 4.5 g/cm^3 and 116 GPa, respectively [20].

3.2. Fracture response

The J-integral versus crack extension Δa curves are shown in Fig. 3 for titanium foams with relative densities of 0.30 and 0.40. The crack blunting lines on the J–Δa plots are given by Eq. (6), where σ_{ys} is the tensile yield strength of the foam.

$$J = 2\sigma_{ys}\Delta a \tag{6}$$

where these blunting lines intercept the J-curve, a conditional value of J_{IC} was found. The J_{IC} for relative density of 0.40 was 2.4 kJ/m^2 and for relative density of 0.30 was 1.3 kJ/m^2. By using Eq. (1), the plane strain fracture toughness (K_{IC}) was found to be 7.0 MN m$^{-3/2}$ for $\bar{\rho} = 0.40$ and 4.0 MN m$^{-3/2}$ for $\bar{\rho} = 0.30$. In comparison, the K_{IC} of

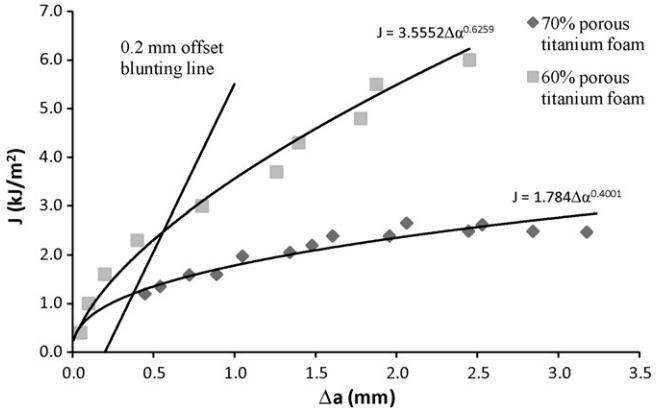

Fig. 3. J-curve for compact tension titanium foams with relative densities of $\bar{\rho} = 0.40$ (60% porous) and $\bar{\rho} = 0.30$ (70% porous). The crack length measurement is carried out using unloading compliance.

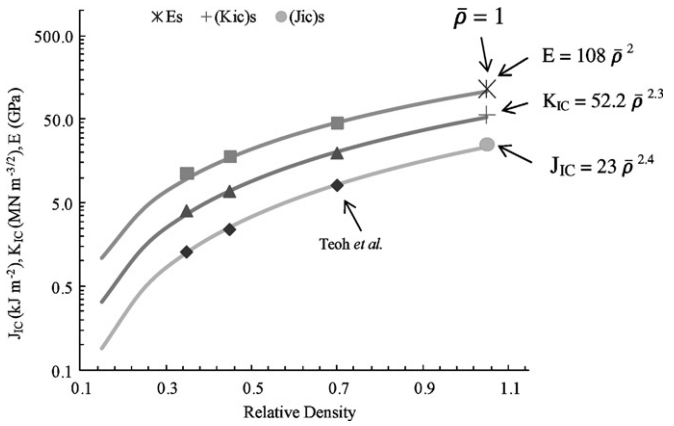

Fig. 4. Effect of relative density on E, K_{IC}, and J_{IC} of titanium foams, using power law fits ($A = B\bar{\rho}^{c}$).

solid pure titanium is 75 (±11) MN m$^{-3/2}$ [21], which is significantly higher.

3.3. Data analysis of power law

An important parameter of the metal foams, which may affect the initiation toughness, is their relative density. The initiation toughness J_{IC} measured from experimental results based on ASTM E1820-08 is shown in Fig. 4. In addition to J_{IC}, the Young's modulus E and also the values of plane strain fracture toughness K_{IC} are shown in Fig. 4. As relative density increases, the values of J_{IC}, K_{IC} and E also increase. The maximum values for these parameters were obtained at $\bar{\rho} = 1$ which corresponds to solid titanium ($(J_{IC})_s$, $(K_{IC})_s$, E_s) [22].

Various types of curve fit could be used to represent the experimental data in Fig. 4; however, the best fit is obtained with power law ($A = B\bar{\rho}^{c}$) for all three properties (J_{IC}, K_{IC} and E). This illustrates that as $\bar{\rho} \to 1$, J_{IC}, K_{IC} and E increase towards their maximum possible values (corresponding to titanium solid). In case of Young's modulus E, a polynomial curve fit could also be used to represent high relative densities, but at lower relative densities polynomial functions predict unexpectedly high values for E, which is unrealistic for a foam material. In addition to relative densities of 0.40 and 0.30, the toughness value for relative density of 0.65 obtained from a study by Teoh et al. [9] follows the power law trend as shown in Fig. 4. The power law fit had also been used and shown to be valid for aluminum foams by McCullough et al. [23].

4. Discussions

4.1. R-curve behavior and crack bridging

The toughness testing on compact tension specimens showed a considerable R-curve behavior. There are two types of factors affecting the R-curve. The first one is the intrinsic factors which are due to the base material properties, its inclusions and impurities. The other is the extrinsic parameters which are due to foam properties such as relative density, morphology and complexity of cell structures behind the crack tip, in the surrounding areas and in the crack wake. The toughening mechanism due to extrinsic factors causes a reduction on the stresses at the crack tip by sustaining part of the applied load, and consequently resisting the crack growth. The scales of strain in these fracture toughness tests verified that the titanium foams have good ductility besides some plastic collapse crosswise the ligaments.

The J-tests confirmed that the crack bridging ligament was present in the beginning of the advancing crack tip and cell faces failed in advance of the crack tip. The crack bridging phenomenon

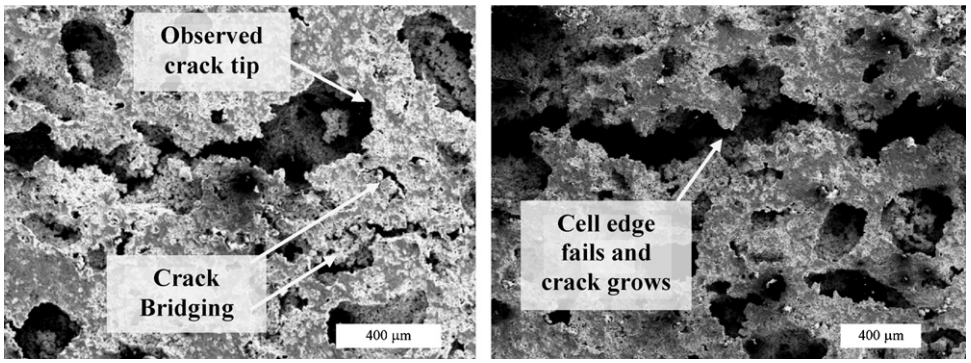

Fig. 5. SEM images of compact tension specimens of 60% porous titanium foams.

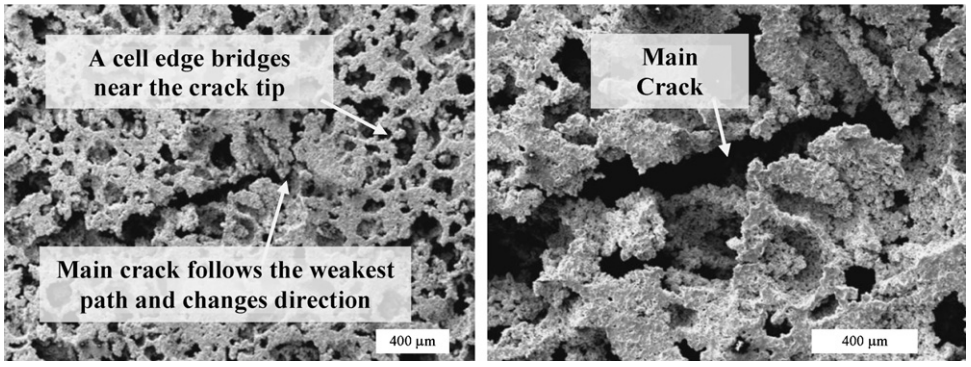

Fig. 6. SEM images of compact tension specimens of 70% porous titanium foams.

could be the primary cause of the R-curve behavior here. The crack bridging is caused by regions of uncracked material spanning the crack wake. As the main crack advances non-uniformly and micro-cracks link imperfectly, the bridging happens in the form of uncracked struts or cell wall faces that are left behind the crack tip.

4.2. Micrographs of compact tension titanium foams

In toughness tests, after a peak load, there were some cracks around the edge corners of the notch tip. The same feature had been seen in closed-cell Alporas and Alulight foams by McCullough et al. and Olurin et al. [23–25]. After a certain number of cycles, a dominant crack spreads down the centerline. This crack seemed to follow the weakest path. Scanning electron microscope (SEM) images are shown in Figs. 5 and 6 for a crack propagating in titanium foams with relative densities of 0.30 and 0.40, respectively. These images show that ahead of the observed crack tip, the failure of cell faces is apparent. Since the crack tip was established by damaged foam, it was difficult to be very exact about the location of the crack tip.

4.3. Comparison of titanium foam's fracture toughness to different materials

For evaluating this porous material for different purposes, the toughness results are compared against some skeletal parts [26–29] for biomedical applications. Porous titanium foams with relative densities of 0.40 (K_{IC} = 7 MN m$^{-3/2}$) and 0.30 (K_{IC} = 4 MN m$^{-3/2}$) have higher toughness values, although similar in order of magnitude, to K_{IC} of cancellous bone (1.5 MN m$^{-3/2}$) and dentine (2.5 MN m$^{-3/2}$) [27,28]. K_{IC} of cortical bone (3.5 MN m$^{-3/2}$) [26,29] is very close to K_{IC} of porous titanium foams with relative density of 0.30.

Titanium foams present a favorable combination of mechanical properties and fracture toughness that make them suitable as structural implant materials for bone replacement.

5. Conclusions

The fracture toughness of titanium foams have been measured and explained in terms of morphology. It is known that data which result in J_{IC} value is independent of in-plane dimensions of the specimen. In this range of relative densities, the titanium foam with higher $\bar{\rho}$ (lower porosity) is tougher than the titanium with lower $\bar{\rho}$ (higher porosity). This shows that the plane strain fracture toughness increases with relative density. Also, the compact tension titanium specimens have some plastic collapse along the ligament. Titanium foams with densities between $0.30 < \bar{\rho} < 0.40$ not only have a matched stiffness to various body parts such as dentine and cancellous bone [7], but also seem to be appropriate choice for implant's material selection from fracture toughness point of view.

Acknowledgements

This work is financially supported by the Australian Research Council (Project No: DP0770021) and ARC grant from ARNAM. The authors also thank David Dick for his support in the E-CORE laboratory.

References

[1] Y.H. An, in: Y.H. An, R.A. Draughn (Eds.), Mechanical Testing of Bone and the Bone–Implant Interface, CRC Press LLC, Florida, USA, 2000, pp. 41–64.
[2] B. Van Rietbergen, R. Huiskes, 51st Annual Meeting of the Orthopaedic Research Society, 2005.
[3] H.A. Mansour, J.D. Ray, D.P. Mukherjee, 14th Southern Biomedical Engineering Conference, Shreveport, Louisiana, 1995.
[4] A. Gefen, Med. Biol. Eng. Comput. 40 (2002) 311–322.
[5] M.G. Dunn, in: T.D. Fahey (Ed.), Encyclopedia of Sports Medicine and Science, 1998.
[6] R.M. Pilliar, H.U. Cameron, A.G. Binnington, J. Szivek, I. Macnab, J. Biomed. Mater. Res. 13 (1979) 799–810.
[7] S. Kashef, W. Yan, J. Lin, P.D. Hodgson, Mod. Phys. Lett. B 22 (2008) 6155–6160.
[8] T. Imwinkelried, J. Biomed. Mater. Res. A (2007) 964–970.
[9] S.H. Teoh, R. Thampuran, W.K.H. Seah, J.C.H. Goh, Biomaterials 14 (6) (1993) 407–412.
[10] M. Takemoto, S. Fujibayashi, M. Neo, J. Suzuki, T. Kodubo, T. Nakamura, Biomaterials 26 (2005) 6014–6023.
[11] H. Shen, S.M. Oppenheimer, D.C. Dunand, L.C. Brinson, Mech. Mater. 38 (2006) 933–944.
[12] S.M. Oppenheimer, D.C. Dunand, Mater. Sci. Eng. A A523 (2009) 70–76.
[13] Z. Esen, S. Bor, Scripta Mater. 56 (2007) 341–344.
[14] C. Yasumasa, D.C. Dunand, Acta Mater. 56 (2008) 105–113.
[15] C.E. Wen, Y. Yamada, A. Nouri, P.D. Hodgson, Mater. Sci. Forum 539–543 (2007) 720–725.
[16] K. Ishizaki, S. Komarneni, M. Nanko, Porous Materials, Process Technology and Applications, Kluwer Academic Publishers, Dordrecht, The Netherlands, 1998.
[17] ASTM E1820-08, Standard Test Method for Measurement of Fracture Toughness, ASTM International, West Conshohocken, PA, USA, 2008.
[18] H. Tada, P.C. Paris, G.R. Irwin (Eds.), The Stress Analysis of Cracks, American Society of Mechanical Engineers, 2000.
[19] M.F. Ashby, A.G. Evans, N.A. Fleck, L.J. Gibson, J.W. Hutchinson, H.N.G. Wadley, Metal Foams: A Design Guide, Butterworth-Heinemann, Woburn, MA, USA, 2000.
[20] N.E. Dowling (Ed.), Mechanical Behaviour of Materials, Engineering Methods for Deformation, Fracture, and Fatigue, Pearson Prentice Hall, Upper Saddle River, NJ, 2007, p. 912.
[21] R.P. Walsh, R.R. Mitchell, V.T. Toplosky, R.C. Gentzlinger, Low temperature tensile and fracture toughness properties of SCRF cavity structural materials, Santa Fe, in: IX Workshop on RF Superconductivity, 1999.
[22] G.T. Hahn, M.F. Kanninen, A.R. Rosenfield, Annu. Rev. Mater. Sci. 2 (1972) 381–404.
[23] K.Y.G. McCullough, N.A. Fleck, M.F. Ashby, Acta Mater. 47 (8) (1999) 2331–2343.
[24] O.B. Olurin, K.Y.G. McCullough, N.A. Fleck, M.F. Ashby, Int. J. Fatigue 23 (2000) 375–382.
[25] O.B. Olurin, N.A. Fleck, M.F. Ashby, Mater. Sci. Eng. A A291 (2000) 136–146.
[26] T.L. Norman, D. Vashishth, D.B. Burr, J. Biomech. 28 (3) (1995) 309–320.
[27] J. Yan, B. Taskonak, J.J. Mecholsky Jr., J. Mech. Behav. Biomed. Mater. 2 (2008) 478–484.
[28] C. Ohman, M. Baleani, E. Perilli, E. Dall'Ara, S. Tassani, F. Baruffaldi, M. Viceconti, J. Biomech. 40 (2007) 2426–2433.
[29] J. Yan, J.J. Mecholsky Jr., K.B. Clifton, Bone 40 (2007) 479–484.